*International Journal of Mining and Geological Engineering*, 1986, **4**, 197–216

# The determination of *in situ* rock thermal properties and the simulation of climate in an underground mine

P. MOUSSET-JONES[1] and M.J. McPHERSON[2]

[1]*Department of Mining Engineering, Mackay School of Mines, University of Nevada, Reno, Nevada 89557, USA*
[2]*Department of Materials Science and Mineral Engineering, University of California, Berkeley, California 94720, USA*

Received 10 January 1986

## Summary

This paper describes the results from a continuing research project started in 1984, which is investigating improved methods for predicting the underground climate in hot mines. The Homestake Gold Mine in South Dakota was the site for testing methods, based on radial heat flow theory, to measure *in situ* values of the thermal conductivity and diffusivity of rock. The methods used proved to be quite within the capability of mine staff to carry out for themselves. The results were acceptable and verified that *in situ* thermal rock properties can differ considerably from laboratory determined values, in this case by a factor of approximately two.

A mine climate simulation program, CLIMSIM, was applied to case studies from the Homestake mine using the measured thermal rock parameters. The results showed good correlation between the measured and simulated values.

*Keywords: In situ* rock conductivity; *in situ* rock diffusivity; mine climate simulation; CLIMSIM, diesel heat output.

## Introduction

During 1984–86, the USBM Mining Systems and Ground Control Generic Research Center in the United States funded a project to investigate improved procedures for planning the airflow and refrigeration requirements in underground mines experiencing hot working conditions. The project was broken down into five phases.

(1) Visiting some of the known hot mines in the US, and sending out a questionnaire to determine which other mines might experience hot working conditions in the future.

(2) Choosing two mines in which to conduct measurements to determine the *in situ* rock thermal conductivity and diffusivity, and comparing these values with laboratory determined values.

0269–0136/86 $03.00+.12 

(3) Investigating computer programs available for mine climate simulation, and testing these programs with case study examples from the two mines where the rock thermal properties were measured.

(4) Considering improved ways of estimating the wetness factor and experimenting with the use of heat flux meters to measure more directly the rock heat inflow into the airstream.

(5) Applying the results of these investigations to simulate the climate in future mine development and production areas at the two mines.

This paper describes the procedures and results of the *in situ* rock thermal property measurements. In addition it gives a summary of the climate simulation results obtained for case studies involving a level, a decline with an operating LHD (load-haul-dump vehicle), and a ramp leading into a mechanized cut and fill stope at the Homestake Gold Mine in South Dakota, USA.

## *In situ* measurement of thermal conductivity ($k$) and thermal diffusivity ($\alpha$)

The first mine chosen for the *in situ* measurements was the Homestake Gold Mine, Lead, South Dakota. It was not easy to locate good sites for the measurements, since certain optimum criteria were to be met. Compounding the problem was the fact that the mine was at full operating capacity, and it proved quite difficult to find suitable sites that would neither change with regard to air flow throughout the measurement period, nor interfere with production. Table 1 indicates the site criteria needed for the respective measurements. The Homestake mine site turned out to be less satisfactory than originally expected due to some unanticipated problems occurring such as fluctuating airflow, and a discharge of water from a cooling unit flowing through the test site.

The 7700 level (2350 m) at the Homestake mine was chosen for both measurements, and

Table 1. List of site requirements for the measurement of thermal conductivity ($k$) and thermal diffusivity ($\alpha$).

| *Thermal conductivity measurement* | *Thermal diffusivity measurement* |
|---|---|
| 1. An adequate length of drift with minor changes in cross sectional area | 1. Dead end |
| 2. A level drift | 2. Easily bratticed off |
| 3. A consistent airflow of medium quantity | 3. Unused for a reasonable period of time, e.g. approximately 3 months |
| 4. An air temperature increase of approximately 2° C over the length of the test section | 4. Can be ventilated by an auxiliary fan and cooling unit |
| 5. Not much traffic in the drift | 5. Power available |
| 6. Available power | 6. Reasonably dry – no running water |
| 7. Reasonably dry – no running water | 7. Far enough away from any other mine opening to prevent interference with heat flow into the test site |
| 8. No other heat source or sink | 8. No other heat source or sink |

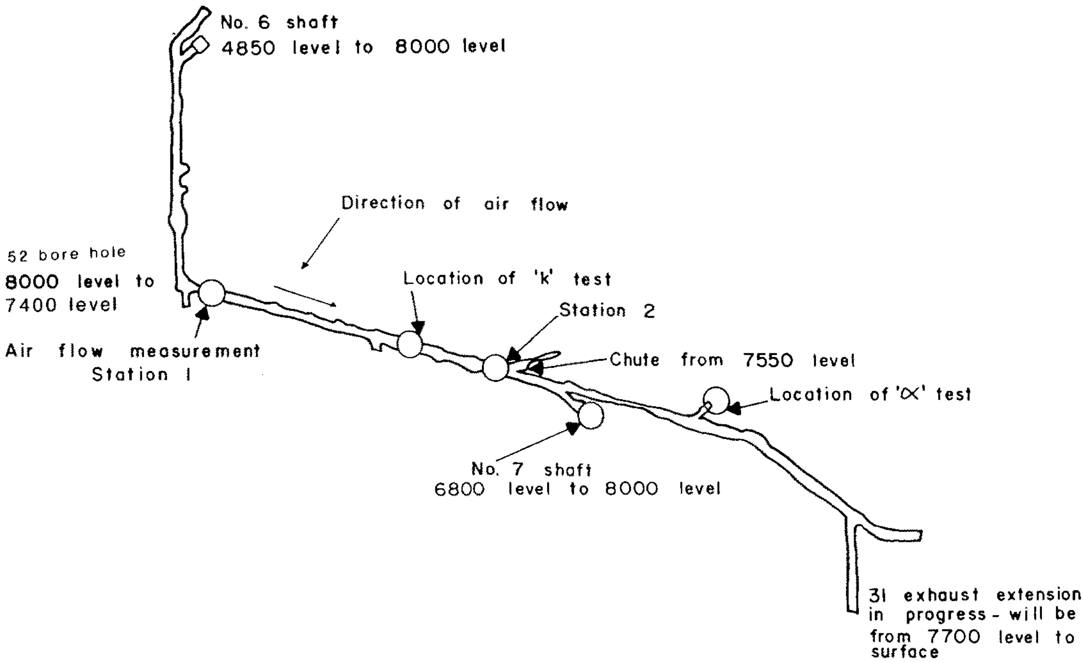


Fig. 1. 7700 level – Homestake Gold Mine (Distance from Station 1 to Station 2 = 247 m).

Fig. 1 illustrates the location of the two sites, which both have similar rock types, namely a fine grained phyllite.

## *Measurement of thermal conductivity* (k)

The procedure for measuring $k$ on the 7700 (2350 m) level at Homestake has been described in previous papers (Mousset-Jones and McPherson, 1983, 1984). Briefly, four 10 m holes were drilled radially from a drift and at right angles to each other. Each hole was instrumented with eight thermocouples, and measurements of airflow, wet bulb and dry bulb temperatures were taken at sites upstream and downstream from the measurement site.

The experimental layout at the $k$ test site is illustrated in Fig. 2. Fig. 3 details the thermocouple string that is a modification of the one used at the Homestake mine. In order to prevent air convection in the drill holes from affecting each thermocouple, styrofoam prills were used to pack each hole. However, this was a troublesome procedure and a new version of each thermocouple probe was made using foam rubber attachments to isolate each thermocouple in the hole as illustrated in Fig. 3. Some preliminary tests have indicated that this system appears to adequately prevent convection in the borehole.

The temperatures measured in one of the holes over the test period are shown in Fig. 4. It can be seen that due to summer warming of the surface air, the first four thermocouples show an increasing temperature starting around June 1984. It is normally unnecessary to carry out *in situ* $k$ measurements over such a long period, since stabilization of the thermocouple readings is all

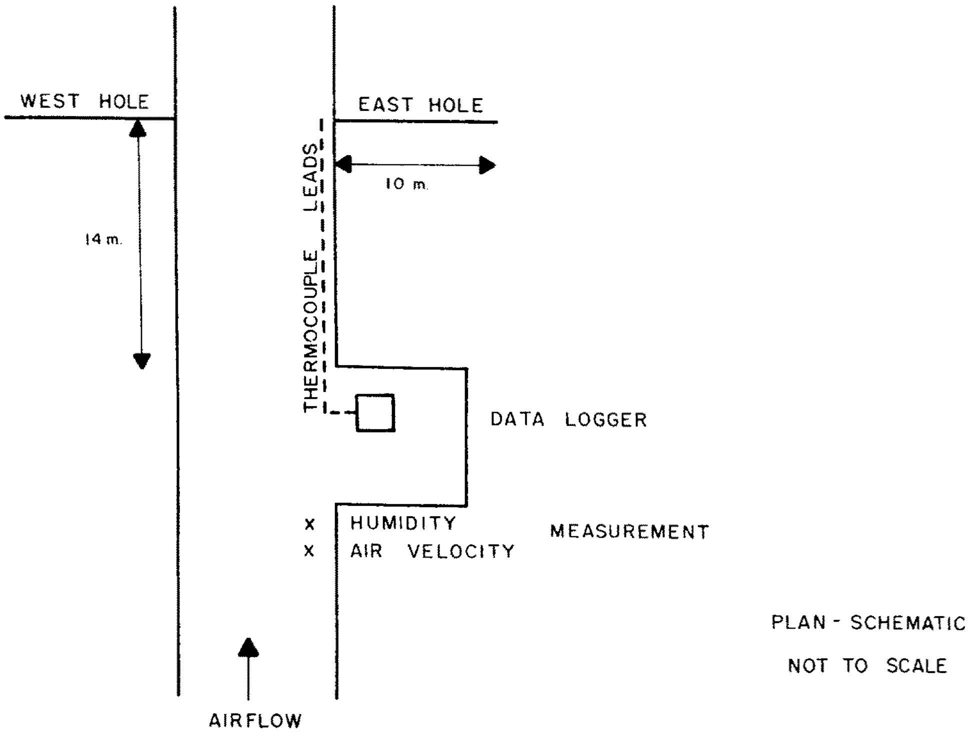


Fig. 2. *In situ k* experiment layout.

that is needed. However in this case it was decided to extend the measurement period to investigate the effect of fluctuating temperatures and airflow.

From these measurements the *in situ* value of $k$ could be calculated by the following procedure (see McPherson, 1986).

At steady state

$$q = \frac{2\pi k L(\theta_2 - \theta_1)\ \mathrm{W}}{\log_e r_2/r_1} \tag{1}$$

where $q$ = radial heat flow (W)
$k$ = thermal conductivity (W $m^{-1\circ}$ $C^{-1}$)
$\theta_i$ = temperature (° C) at location $r_i$ (m) from centre of drift
$L$ = length of airway (m)

In order to determine $q$, the increase in sigma heat of the airflow through the test site has to be calculated. Then the slope of a graph of temperature ($\theta$) against $\log_e$ of distance ($r$) will be

$$\frac{(\theta_2 - \theta_1)}{\log_e \dfrac{r_2}{r_1}} = \frac{q}{2\pi k L} = b^\circ\ C$$

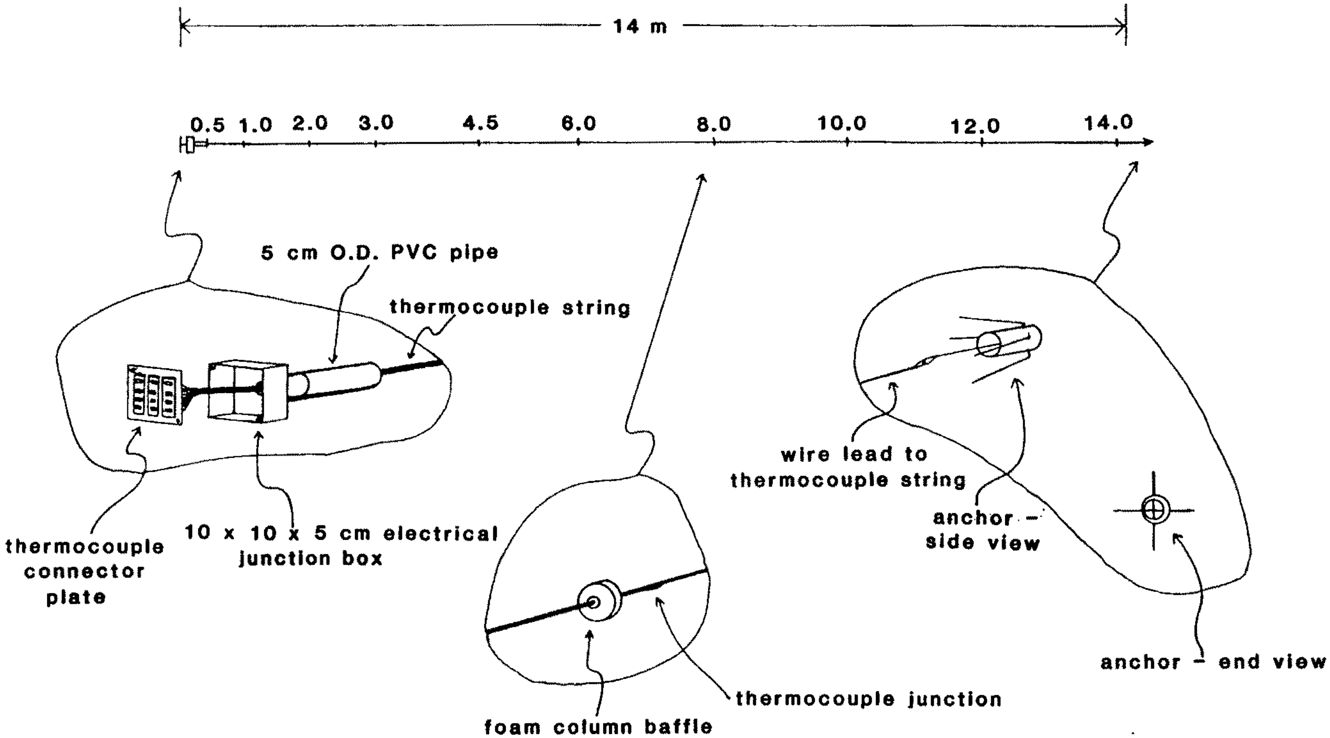


Fig. 3. Thermocouple string.

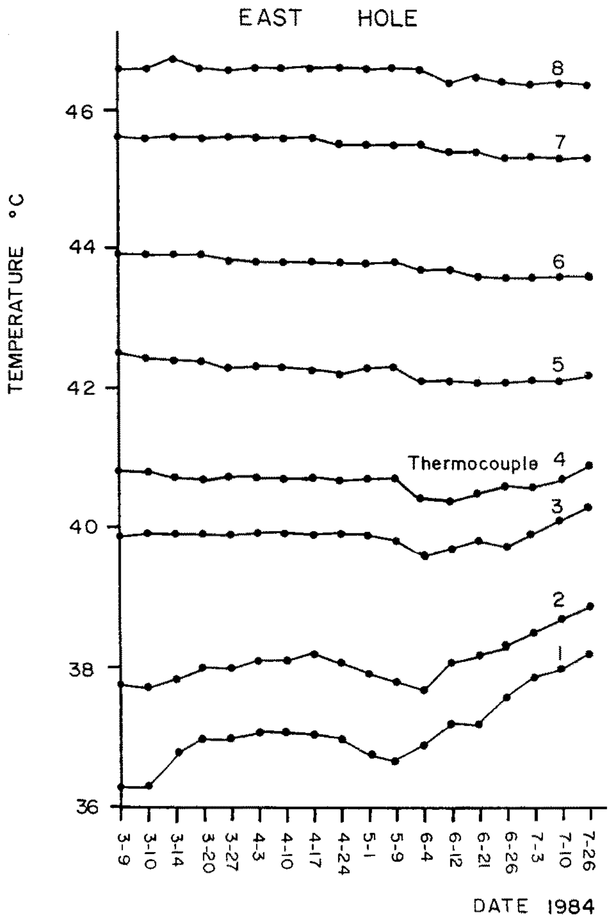


Fig. 4. Thermocouple temperatures over measurement period.

Thus $k = \frac{q}{2\pi L b}$ W m$^{-1\circ}$ C

At the Homestake test, the airway length, $L$, was 247 m, giving

$$k = 0.6444 \times 10^{-3} \times \frac{q}{b} \text{ W m}^{-1\circ} \text{ C}^{-1} \qquad (2)$$

An example of the temperature profiles indicated by the thermocouples in a hole is shown in Fig. 5. It was decided to determine the slopes for the average thermocouple readings recorded on the day of each airflow measurement. For each hole the values of $\theta$ and $r+1.5$ were input into a linear regression program for determination of the slope, $b$, in the equation

$$\theta = b \log_e(r+1.5) + c$$

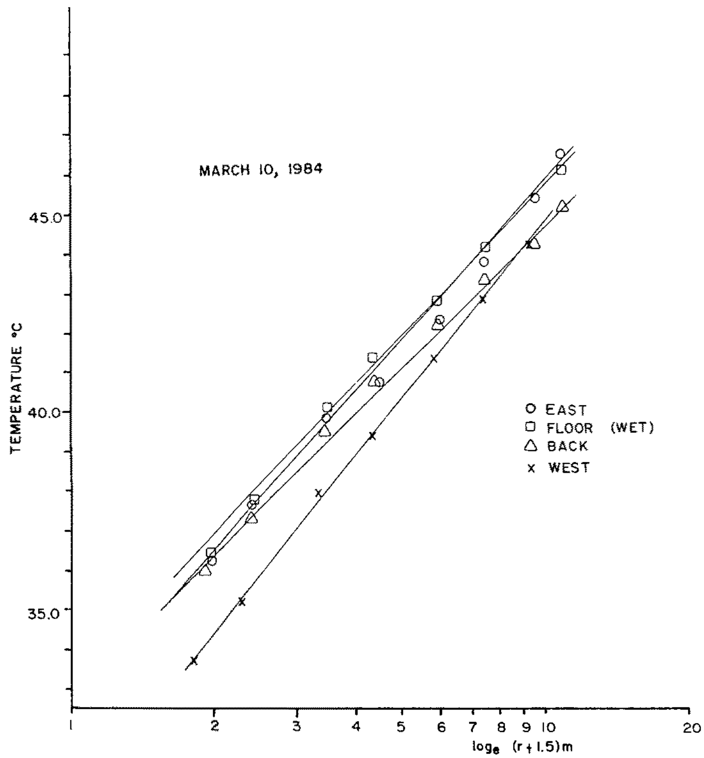


Fig. 5. Temperature profile for test holes using $\log_e$ of the distance $r$.

The additional 1.5 m made allowance for the fact that $r$ was measured from the rock surface rather than the centre line of the airway.

The results of these calculations are shown in Table 2 which tabulates the values of $b$ and $k$ for each hole on each airflow measurement day. The value of $k$ ranges from 3.38 to 6.41 W $m^{-1}$° C with an average of 4.82 W $m^{-1}$° C. A number of different rationales could be used to discard some values as possibly spurious. However, without any really strong justification, it was decided to take the average of all the results as a reasonable indication of the *in situ* thermal conductivity value for the rock on the 7700 (2350 m) level.

## *Laboratory measurement of thermal conductivity*

Laboratory values of $k$ were determined using an unguarded plate apparatus designed by Ashworth and Ashworth (1980) and illustrated in Fig. 6. A copy of this design with minor modifications was built and used to determine values of $k$ for 1.27 cm thick × 10.16 cm diameter samples cored from rock taken from the 7700 (2350 m) level at Homestake. The values obtained were compared with those obtained using a TC 1000 thermal comparator, and other accurate $k$ value test units. A comparison between the values indicate that the heat loss in the unguarded plate apparatus was approximately 5%.

Table 2. Calculation of thermal conductivity ($k$).

| | *East Hole* | | *West Hole* | | *Back Hole* | | *Floor Hole* | | |
|---|---|---|---|---|---|---|---|---|---|
| *Date* | $b$ | $k$ | $b$ | $k$ | $b$ | $k$ | $b$ | $k$ | *Average** $k$ |
| 10 March | 5.775 | 4.730 | 5.565 | 4.91 | 5.042 | 5.42 | 6.569 | 4.16 | 5.02 |
| 27 March | 5.424 | 4.71 | 5.195 | 4.918 | 4.563 | 5.598 | 5.527 | 4.622 | 5.08 |
| 3 April | 5.424 | 6.464 | 5.195 | 7.129 | 4.563 | 5.623 | 5.527 | 6.343 | 6.41 |
| 10 April | 5.424 | 4.823 | 5.195 | 5.036 | 4.563 | 5.733 | 5.527 | 4.733 | 5.20 |
| 17 April | 5.424 | 4.494 | 5.195 | 4.692 | 4.563 | 5.342 | 5.527 | 4.410 | 4.84 |
| 24 April | 5.424 | 4.172 | 5.195 | 4.356 | 4.563 | 4.959 | 5.527 | 4.094 | 4.50 |
| 1 May | 5.508 | 3.620 | 5.268 | 3.784 | 4.802 | 4.152 | 5.741 | 3.473 | 3.85 |
| 4 June | 5.424 | 4.760 | 5.111 | 5.051 | 4.570 | 5.650 | 5.271 | 4.898 | 5.15 |
| 12 June | 5.424 | 3.935 | 5.111 | 4.175 | 4.570 | 3.770 | 5.271 | 4.049 | 3.96 |
| 21 June | 5.145 | 3.557 | 4.791 | 3.820 | 4.225 | 4.331 | 4.926 | 3.715 | 3.90 |
| 26 June | 5.145 | 3.082 | 4.791 | 3.310 | 4.225 | 3.753 | 4.926 | 3.219 | 3.38 |
| 3 July | 4.669 | 4.633 | 4.350 | 4.973 | 3.720 | 5.815 | 4.466 | 4.865 | 5.14 |
| 10 July | 4.669 | 4.424 | 4.350 | 4.749 | 3.720 | 5.553 | 4.466 | 4.625 | 4.91 |
| 26 July | 4.584 | 5.496 | 4.233 | 5.951 | 3.664 | 6.876 | 4.373 | 5.761 | 6.11 |
| | | | | | | | | | Average 4.82 W° $C^{-1}$ |

$b$ = Slope of $\theta/\log_e r$ line
$k$ (W $m^{-1°}$ $C^{-1}$) = Thermal conductivity
*Average of East, West, and Back Hole values of $k$

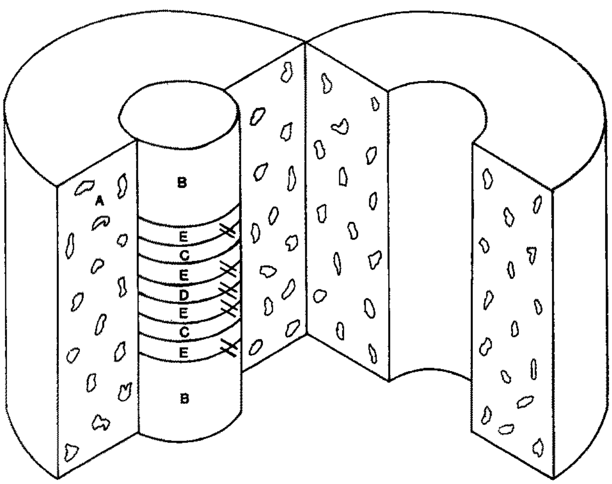


A. Insulation
B. 10.16 cm diameter heat sinks - 20.32 cm long
C. 1.27 cm thick x 10.16 cm diameter rock samples
D. Heater plate, 0.635 cm x 10.16 cm diameter
E. Thermistor plates, 0.476 cm x 10.16 cm diameter

Fig. 6. Unguarded plate column.

Table 3. Laboratory values of thermal conductivity determined by unguarded plate apparatus.

| | *Test No. 1* *Sample against nylon* $k$ (W $m^{-1\circ}$ $C^{-1}$) | *Test No. 2* *Sample against like sample* $k$ (W $m^{-1\circ}$ $C^{-1}$) |
|---|---|---|
| Nylon | −0.31 | −0.31 |
| D1 | −1.54 | −1.59 |
| D2 | −1.60 | −1.59 |
| S1 | −2.36 | −2.45 |
| S2 | −2.91 | −2.98 |
| S3 | −2.27 | −2.45 |
| K1 | −2.91 | −2.98 |
| K2 | −1.94 | −2.08 |
| K3 | −2.00 | −2.08 |

*5% system heat loss.

The values of thermal conductivity obtained from the laboratory tests shown in Table 3 exhibit considerable scatter. The main cause of the variation is the nature of the rock sample itself. For example, a quartz inclusion, or a microfracture will cause some of the differences noted in this table. In addition, these values were obtained for relatively dry rock samples. The effect of water and stress on the $k$ value of rock can be considerable. A value of approximately 2.6 W $m^{-1\circ}$ $C^{-1}$ was taken as an average of the laboratory determined values compared with 4.82 W $m^{-1\circ}$ $C^{-1}$ measured *in situ*. The reasons for the difference were attributed to the facts that the rock was subject to considerable stress at 2350 m below surface and was also affected by ground water movement in the rock mass. It will be seen later in the paper that a similar but higher value was obtained when calculated from the *in situ* diffusivity. Therefore the average value for the complete level may be even higher than the 4.82 W $m^{-1\circ}$ $C^{-1}$ that was measured at one single cross section.

Based on these results the *in situ* value was 1.85 times the value obtained in the laboratory. This was an important finding since it verified the expected difference between the two values. In addition, it showed that it may well be worthwhile for a mine to make an effort to obtain reasonably accurate values, i.e. $\pm 5\%$, for *in situ* rock thermal properties.

### *Measurement of thermal diffusivity ($\alpha$)*

*Theoretical discussion.* The method used at Homestake followed the procedure developed by Vost (1976). Briefly it involved drilling holes 15 m radially outwards from the side of a dead end drift and instrumenting each hole with a string of thermocouples or thermistors. The dead end drift was then closed off with a bulkhead and allowed to heat up so that the surface rock temperatures of the drift approached virgin rock temperature (VRT). Then the bulkhead was opened up and the drift ventilated, so that the impact of the cooling down process on the rock temperature in the holes could be continuously recorded, until there was no further change in the rock temperatures measured in the holes. These measurements were then compared with simulated values of temperature at similar locations in the hole for various values of diffusivity.

The value that gave the best correlation was then considered to be the most likely *in situ* value of $\alpha$.

The two heat flow equations used by Vost and simulated using forward difference approximation are as follows:

$$\text{Linear flow } \frac{\partial^2 \theta}{\partial x^2} = \frac{1}{\alpha} \frac{\partial \theta}{\partial t} \tag{3}$$

$$\text{Radial flow } \frac{\partial^2 \theta}{\partial r^2} + \frac{1}{r} \frac{\partial \theta}{\partial r} = \frac{1}{\alpha} \frac{\partial \theta}{\partial T} \tag{4}$$

where $\theta$ = temperature at some point, distance $r$
$r$ = measured radially outwards into the rock from the axial centre line of the airway (m)
$T$ = dimensionless time = $\alpha t / r_a^2$ or
$x$ = distance between any two points in the rock (m)
$t$ = time (s) since the surface was exposed
$\alpha$ = thermal diffusivity ($m^2\ s^{-1}$)
$r_a$ = airway radius (m)

The forward difference approximation of linear flow has been described in previous papers (Starfield *et al.*, 1964; Vost, 1976). See Appendix 1 for an explanation of the method for radial flow.

*Implementation*

The site detail on the 7700 (2350 m) level, and the position of the thermocouples within the side hole are illustrated in Fig. 7. Unfortunately it proved impossible to heat up the dead end to VRT. This was due mainly to two reasons, firstly the bulkhead consisted of a single layer brattice, which in addition did not fit tightly around the perimeter of the rock surface. Secondly, the drift was a short crosscut, only 40 m in length from the main level. This meant that the rock temperatures in the crosscut were undoubtedly affected by the proximity of the main level.

Notwithstanding these difficulties, the crosscut did indeed heat up reasonably well and in July 1984 the brattice was removed for subsequent cooldown and a continuous record was made of rock temperature variation in the hole for a period of 94 days. As the rock cooled down, some further problems were encountered, firstly trouble with the paper jamming in the data logger, which was not noticed for a few days since only one visit per week could be made by the ventilation engineer. Secondly, the temperature difference between the air in the 7700 (2350 m) level and the crosscut was only about 5° C, hence the cooling down was very slow. In fact, near the end of the measurement period the 7700 (2350 m) level heated up due to higher surface air temperature because it was summertime. However, a period of 51 days was obtained where a continuous unbroken decline in thermocouple temperatures was observed for all the thermocouples in the hole. The temperatures recorded for this 51 day period were used as a basis for the simulations, and against which the simulated values were compared.

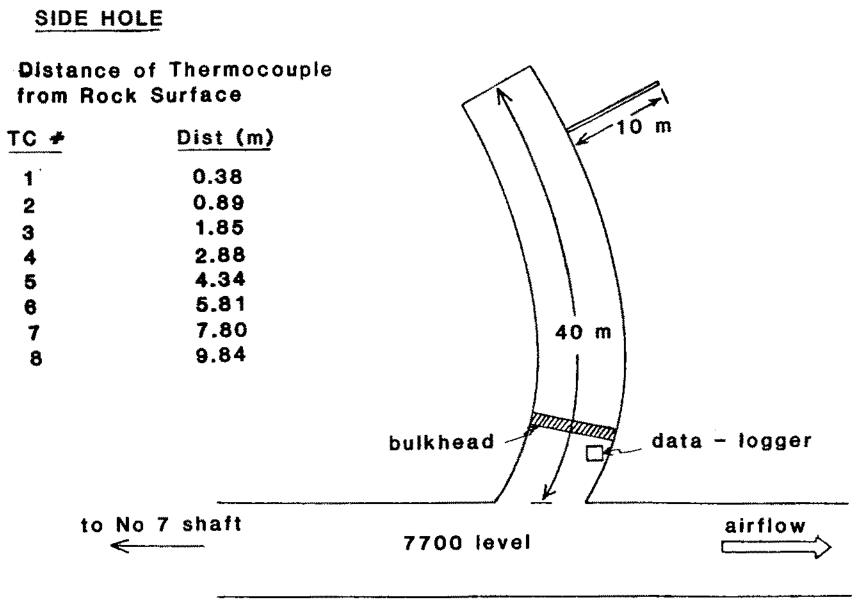


Fig. 7. Layout of test site on 7700 level – Homestake Mine (not to scale).

## Results

A large number of diffusivity computations were run with a number of difficulties encountered due to the sensitivity of the forward difference approximation to changes in $\Delta t$, $\Delta r$, and $\Delta x$. Since this simulation was for a period of 51 days, attempts were made to increase the increment of time ($\Delta t$) but this led to erroneous, cyclic, or totally meaningless results. This also occurred for too large values of incremental distance ($\Delta r$, $\Delta x$). Hence to obtain a good set of results required the full storage capacity of a CDC 730 computer and a considerable amount of computer time to simulate results for a whole range of $\alpha$ from $0.1 \times 10^{-6}$ to $0.3 \times 10^{-5}$ $m^2 s^{-1}$.

### *Side hole – radial*

Average specific heat ($C$) and density ($\rho$) values determined for rock samples taken from the 7700 (2350 m) level were respectively 807.8 J $kg^{-1} {}^\circ C^{-1}$ and 2.83 g $cm^{-3}$.

Using these values a value of $\alpha$ was calculated from the following equation, using the average *in situ* value of $k$ previously determined as 4.82 W $m^{-1} {}^\circ C^{-1}$.

$$\alpha = \frac{k}{\rho C} = \frac{4.82}{2830 \times 807.8} = 0.21 \times 10^{-5}\ m^2\ s^{-1} = 0.00759\ m^2\ h^{-1}$$

This value of $\alpha$ was used as a starting value for the simulation algorithm. The values for the six central thermocouples were simulated using the first and last thermocouple readings as reference values for the simulation at each time interval. Least square fits were calculated between the simulated and actual values for the central six thermocouple temperature readings. The fit improved with increasing values of $\alpha$ beyond $0.21 \times 10^{-5}$ m$^2$ s$^{-1}$, and became worse with decreasing values of $\alpha$. A best fit was obtained at the value of $0.27 \times 10^{-5}$ m$^2$ s$^{-1}$, and assuming that $C$ and $\rho$ are correct, this was used to calculate a value of $k$ of 6.17 W m$^{-1\circ}$ C$^{-1}$, which is within the range of measured *in situ* values. Fig. 8 shows the graph obtained for the simulation results. Using a diffusivity value of $0.27 \times 10^{-5}$ m$^2$ s$^{-1}$ gave agreement between simulated and observed rock temperatures within 0.1° C for the majority of the thermocouples, and none more than 0.2° C.

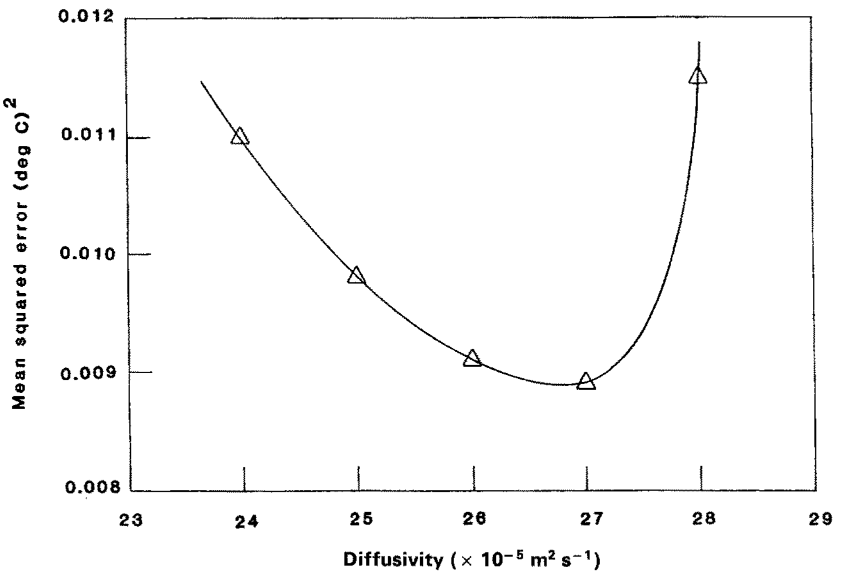


Fig. 8. Mean squared error fit for diffusivity – side hole, radial flow.

This result was encouraging and appears to indicate that radial heat flow theory is applicable to estimating an *in situ* $\alpha$ value. Using the measured values of $C$ and $\rho$ to calculate $\alpha$ from both laboratory and *in situ* values of $k$, the following results are obtained:

Laboratory $k$ value: $\alpha = 0.12 \times 10^{-5}$ m$^2$ s$^{-1}$
*In situ* $k$ value: $\alpha = 0.21 \times 10^{-5}$ m$^2$ s$^{-1}$
*In situ* measured: $\alpha = 0.27 \times 10^{-5}$ m$^2$ s$^{-1}$

The *in situ* $\alpha$ value is 2.25 times the value obtained in the laboratory, indicating the significant difference between the two values similar to that determined for $k$. Difficulties were encountered with the diffusivity simulation using linear flow theory, indicating that in this particular measurement layout, i.e. the position of the sidehole relative to the end of the crosscut, radial theory works best. It is anticipated that the closer the sidehole is drilled to the end of the crosscut, the less likely that radial theory will work, and possibly linear theory will become more applicable. This trend needs to be further investigated.

**Climatic simulation verification tests**

*The 7700 level*

During the twenty week period of the thermal conductivity experiment at Homestake, repeated measurements of airflows and temperatures were taken at the inlet and outlet ends of the 247 m test length. This offered an excellent opportunity of examining the reliability of the CLIMSIM Program (see McPherson, 1986).

The two end sites for airflow and temperature measurements are shown as stations 1 and 2 on Fig. 1. The constants employed for the simulations were as follows:

| | |
|---|---|
| Length | 247 m |
| Cross sectional area | 6.687 $m^2$ |
| Perimeter | 9.786 m |
| Airway friction factor | 0.012 kg $m^{-3}$ |
| Age | 2 years |
| Wetness factor | 0.25 |

(The wetness varied from damp footwalls and sidewalls to standing pools of water.)

| | |
|---|---|
| Virgin rock temperature | 48° C |

(Estimated from extrapolation of borehole temperatures.)

| | |
|---|---|
| Thermal conductivity | 4.82 W $m^{-1}$° $C^{-1}$ |
| Thermal diffusivity | 0.00759 $m^2$ $h^{-1}$ |

During the test period, the airflow varied from 2.98 to 7.38 $m^3$ $s^{-1}$. For the first nine weeks, an uncovered drainage channel carried cold water returning from a heat exchanger. The heat removed by this cooling source was calculated as

$$q_w = M_w C_w \Delta t \quad \text{kW}$$

where $M_w$ = mass flow of water — kg $s^{-1}$

$C_w$ = specific heat of water — 4.187 kJ $kg^{-1}$° $C^{-1}$

and $t$ = rise in temperature of the water — ° C

This heat transfer was entered into the program runs as a negative linear heat source distributed along the 247 m length. Simulations were carried out for 14 sets of observations.

The temperatures predicted by CLIMSIM were compared with the actual measurements. Despite the variability of the airflow and cooling source, all wet bulb temperatures were predicted to within 0.5° C of observed values. The average error was 0.14° C while the average of absolute errors (disregarding sign) was 0.17° C. The dry bulb temperatures showed greater variation. This is usually the case and is a result of deviations in rates of evaporation. The errors in dry bulb temperature varied from −0.9 to 1.1° C with an average of 0.05° C. The mean of absolute errors was 0.58°C. It is observed that all the errors in dry bulb temperature were negative (i.e. CLIMSIM predictions slightly less than measured values) during the time that the cold water channel was in operation. However, following the cessation of this cold source, all but the first successive simulation gave a positive error in the dry bulb temperature. This may have been caused by condensation on the cold water surface. However the deviations between predicted and measured temperature were sufficiently small that a discussion on their causes may be somewhat academic.

*The ramp tests with diesels*

At the time of the initial simulation trials at Homestake, the CLIMSIM program treated all machines as producing sensible heat only. This had given satisfactory results in numerous previous correlations at other mines involving electrical equipment. However, when applied to a working area that included diesels at Homestake, CLIMSIM produced dry bulb temperatures that were much too high. In contrast, the wet bulb temperatures were predicted accurately, indicating that the net heat addition from machines and the strata was properly simulated. Such a situation is normally symptomatic of an inaccurate wetness factor. However, in this case, sensitivity runs indicated that a wetness factor in excess of unity would be required to produce the observed dry bulb temperatures. This can occur only in conditions of forced evaporation such as may be produced by sprays, wet fill, or the wetting down of newly broken rock.

It was realized that the increased moisture content of the air and, hence, the reduced actual rate of dry bulb temperature rise was a result of water vapour produced by the diesels. It was this experiment that led to the program being further developed in order to handle diesel equipment. (See the section on *Additional sources of heat and moisture* in the accompanying paper, 'The analysis and simulation of heat flow into underground airways.')

The rate at which diesel equipment emits water vapour appears to be highly variable. A minimum base value is the water vapour produced as a result of the combustion of fuel. However, additional evaporation takes place from cooling systems and exhaust scrubbers. Table 4 gives some individual items. The total vapour output is the sum of all emitting sources on any given machine. Psychrometric measurements made across diesels at Homestake and carried out by the mine ventilation personnel indicated a total of 9 l water (liquid equivalent) per l fuel consumed.

Table 5 gives a summary of two tests made in an access decline to a cut and fill stope, and indicates excellent predictions by CLIMSIM when using the value of 9 l water per l diesel fuel.

Table 4. Water vapour produced by components of diesel engines.

| *Source* | *Litres of water per litre of fuel per hour** | *Litres of water per rated kW per hour* |
|---|---|---|
| LHD Manufacturer (US) (from fuel only) | 1.46 | 0.44 |
| Kibble (UK) (from fuel only) | 1.1 | 0.33 |
| CANMET (Canada) (fuel and water emulsification) | 0.83 | 0.25 |
| Burgwinkel (West Germany) (fuel and scrubber) | 3.33 | 1.0 |
| MSHA (US) requirement for capacity of exhaust scrubbers | 3.83 | 1.15 |

*Based on a mean fuel consumption of 0.3 litres of fuel per rated kW per hour.

Table 5. Summary of CLIMSIM correlation tests in a decline with operating diesels.

| | |
|---|---|
| Airflow | 5.14 $m^3\ s^{-1}$ |
| Virgin rock temperature at inlet | 35.5° C |
| Geothermal step | 45.7 m° $C^{-1}$ |
| Water vapour produced by diesels | 9 litres (liquid equivalent) per litre of fuel |
| Vertical displacement between stations | 5 m |
| Test 1 | |
| Rated diesel power | 112 kW |
| Percentage utilization | 20 |
| Upstream wet bulb/dry bulb | 24.3/26.7° C |
| Downstream wet bulb/dry bulb | 26.8/30.8° C |
| CLIMSIM predicted downstream wet bulb/dry bulb | 26.9/30.7° C |
| Test 2 | |
| Rated diesel power | 53 kW |
| Percentage utilization | 35 |
| Upstream wet bulb/dry bulb | 24.3/26.7° C |
| Downstream wet bulb/dry bulb | 26.5/30.3° C |
| CLIMSIM predicted downstream wet bulb/dry bulb | 26.5/30.1° C |

### *Practical mine application*

The mine ventilation engineer at the Homestake gold mine needs to estimate the cooling requirements for the many cut and fill stopes which are constantly moving through the production and fill cycles. The climate of currently operating stopes can be directly measured, and cooling needs calculated. However for long term planning of cooling requirements, it is necessary to estimate what will be needed for future stopes.

In order to assist this process CLIMSIM was tested to see how well it could predict the air temperatures entering a stope. The layout of a typical stope showing the normal cooling

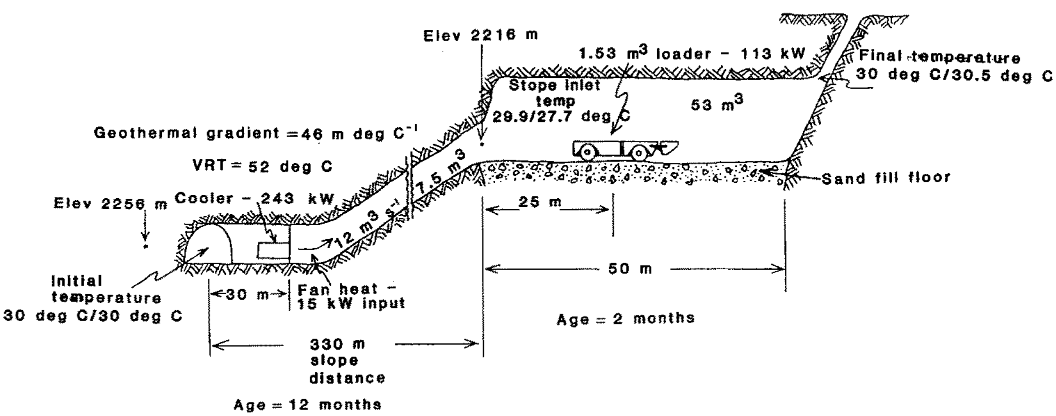


Fig. 9. Layout of mechanized cut and fill stope – Homestake Mine (not to scale).

arrangement for conditioning the air prior to entering the stope is illustrated in Fig. 9. Table 6 is an example of the output which shows that CLIMSIM predicted that the air temperatures at inlet for the stope would be 29.93–27.79° C, which compared favourably with measured values. This illustration shows how CLIMSIM can be used in a very practical manner to provide the mine ventilation engineer with the necessary information for long term planning.

At the present time there is no computer program available which is designed to simulate the climate in a cut and fill stope. The major problems to be overcome are how to deal with (1) the irregular shape; (2) the anisotropic heat flux distribution; and (3) the effect of the fill. It is hoped that future research will result in such a program so that the climate can be simulated for the complete stope cycle.

Table 6. Output from CLIMSIM program. Stope inlet.

*Initial parameters for the prediction of heat and humidity*

Physical description of roadway
Length = 330 m, depth in = 2256 m, depth out = 2216 m, cross-sectional area = 7.5 m

Ventilation at intake
Quantity = 12 ($m^3 s^{-1}$), pressure = 109.4 (kPa), wet bulb temperature = 30° C, dry bulb temperature = 30° C

Thermal parameters
VRT at inlet = 52° C, geothermal step = 46 m° $C^{-1}$, conductivity = 4.820 W $m^{-1}$° $C^{-1}$, diffusivity = 0.007600 $m^2 h^{-1}$, airway friction coefficient = 0.012 kg $m^{-3}$, wetness factor = 0.2, heat transfer coefficient = 67.968 kJ $h^{-1}$ $m^{-1}$° $C^{-1}$

Age = 8760 h = 1 year
Distance between temperature outputs = 50 m

Plant

| *Number* | *Distance (m)* | *Power (kW)* | *Length (m)* |
|---|---|---|---|
| 1 | 30 | −228.0 | |

*Predicted environment*

| *Station number* | *Distance (m)* | *Dry bulb temp (°C)* | *Wet bulb temp (°C)* | *Moisture content* | *Relative humidity* | *Enthalpy (kJ)* | *Effective temp* | *acp ($W m^{-2}$)* | *Pressure (kPa)* | *Density ($kg m^{-3}$)* | *VRT (°C)* |
|---|---|---|---|---|---|---|---|---|---|---|---|
| 0 | 0 | 30.00 | 30.00 | 0.0251 | 1.000 | 94.24 | 26.78 | 383 | 109.400 | 1.2383 | 52.0 |
| After spot source no. 1 power −228 | | | | | | | | | | | |
| 1 | 47 | 26.61 | 26.61 | 0.0205 | 1.000 | 78.90 | 21.83 | 598 | 109.329 | 1.2383 | 51.9 |
| 2 | 94 | 27.34 | 26.81 | 0.0205 | 0.960 | 79.83 | 22.57 | 602 | 109.257 | 1.2548 | 51.8 |
| 3 | 141 | 27.99 | 27.02 | 0.0206 | 0.928 | 80.73 | 23.22 | 588 | 109.185 | 1.2509 | 51.6 |
| 4 | 189 | 28.56 | 27.22 | 0.0207 | 0.902 | 81.62 | 23.79 | 574 | 109.113 | 1.2473 | 51.5 |
| 5 | 236 | 29.07 | 27.42 | 0.0209 | 0.880 | 82.48 | 24.29 | 560 | 109.041 | 1.2440 | 51.4 |
| 6 | 283 | 29.52 | 27.61 | 0.0210 | 0.863 | 83.32 | 24.73 | 548 | 108.969 | 1.2410 | 51.3 |
| 7 | 330 | 29.93 | 27.79 | 0.0212 | 0.848 | 84.15 | 25.13 | 535 | 108.898 | 1.2382 | 51.1 |

## Conclusions

The methods for measuring *in situ* values of thermal conductivity, $k$, and diffusivity, $\alpha$, appear to work well and can be carried out by a mine ventilation engineer. A significant finding is the fact that the measured *in situ* values of $k$ and $\alpha$ were approximately twice the corresponding values obtained in the laboratory. The applicability of linear or radial flow theory to certain measurement site layouts needs to be further investigated. However, provided that the temperature measuring borehole is located an adequate distance from the end of the test drift or crosscut, then radial flow theory can be used with success. It is important to determine the effect of variations in rock thermal properties on the predicted air conditions, since this will indicate the tolerance that is acceptable for the *in situ* values of these parameters.

The CLIMSIM correlation trials indicated good agreement between the predicted and measured values of wet and dry bulb temperatures for a level containing chilled water in a drainage channel, a decline with diesel equipment and an entrance ramp to a cut and fill stope. The simulations at Homestake confirmed the need for correlation trials before climatic simulation is used for planning purposes at any mine. This is achieved by comparing simulated with actual measured temperatures until all significant sources of heat and humidity have been identified and quantified. Since CLIMSIM is an easy program to use, modifications to input data can be made and the results displayed within about one minute. This means that the sensitivity of the final prediction temperatures to changes in input parameters can be quickly and simply achieved. In this way, those parameters which have the greatest impact on the design and economics of the ventilation–cooling system can be pinpointed. It is then for management to decide whether or not it is worthwhile to spend time and money to improve the accuracy of these critical input parameters.

## Acknowledgements

The authors would like to thank the Office of Mineral Institutes, US Bureau of Mines, Grant Number G1125151 for its support of this project. The assistance of the mine management and in particular Mr John Marks at Homestake was invaluable, and without it the project could not have taken place. Thanks to Mr Leong Kwa and Mr Peter Lenz, graduate students who assisted in many ways by assembling the equipment and carrying out the computer simulations. Particular thanks go to Dr Vost for his cooperation and interest in the project, by providing advice and a copy of two computer programs so that the simulations could be undertaken. Finally thanks to Professors T. Ashworth and E. Ashworth of the South Dakota School of Mines and Technology who provided the design and checked the unguarded plate apparatus for measuring thermal conductivity.

**Appendix I**

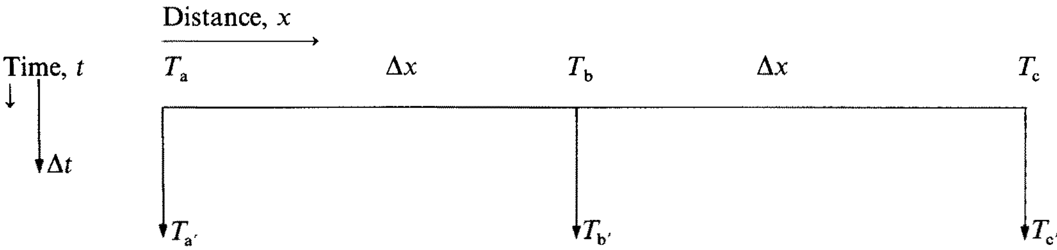


Equation for radial flow

$$\frac{\partial^2\theta}{\partial^2 r}+\frac{1}{r}\frac{\partial\theta}{\partial r}=\frac{1}{\alpha}\frac{\partial\theta}{\partial t} \qquad (1)$$

Consider expansion for $f(x_0+h)$ where $h$ is a small increment.

$$f(x_0+h)=f(x_0)+h\left[\frac{\partial f}{\partial x_0}\right]+\frac{h^2}{2!}\left[\frac{\partial^2 f}{\partial x_0^2}\right]+\ \ldots \qquad (2)$$

similarly,

$$f(x_0-h)=(f(x_0)-h\left(\frac{\partial f}{\partial x_0}\right)+\frac{h^2}{2!}\left(\frac{\partial^2 f}{\partial x_0^2}\right)+\ \ldots \qquad (3)$$

(2)−(3) and disregarding terms greater than $\left(\frac{\partial f}{\partial x_0}\right)$

$$2h\left(\frac{\partial f}{\partial x_0}\right)=f(x_0+h)-f(x_0-h)$$

$$\therefore\ \left(\frac{\partial f}{\partial x_0}\right)=\frac{f(x_0+h)-f(x_0-h)}{2h} \qquad (4)$$

and, (2)+(3)

$$\left(\frac{\partial^2 f}{\partial x_0^2}\right)=\frac{f(x_0-h)-2f(x_0)+f(x_0+h)}{h^2} \qquad (5)$$

Now, consider $f(t_0+n)$'s expansion:

$$f(t_0+n)_0=f(t_0)+n\left(\frac{\partial f}{\partial h}\right)_0+\ \ldots$$

$$\therefore\ \left(\frac{\partial f}{\partial n_0}\right)=\frac{f(t_0+n)-f(t_0)}{n} \qquad (6)$$

Let $h=\Delta r$, $\Delta n=t$, $T_x=f(x)$, $T_t=f(t)$, $T_0=f(x_0, t_0)$
$\therefore$ Equation (4) becomes

$$\left(\frac{\partial f}{\partial r}\right)=\frac{T_c-T_a}{2\Delta r}$$

Equation (5) becomes

$$\left(\frac{\partial^2 f}{\partial r^2}\right)=\frac{T_a-2T_b+T_c}{(\Delta r)^2}$$

and Equation (6) becomes

$$\left(\frac{\partial f}{\partial t}\right)=\frac{T_{b'}-T_b}{\Delta t}$$

Hence, Equation (1) becomes

$$\frac{T_a-2T_b+T_c}{(\Delta r)^2}+\frac{1}{r}\,\frac{T_c-T_a}{2\Delta r}=\frac{1}{\alpha}\left(\frac{T_{b'}-T_b}{\Delta t}\right)$$

Let $m=\dfrac{r}{\Delta r}$ and $S=\dfrac{\alpha\Delta t}{(\Delta x)^2}$

$r$ = distance from centre of drift to thermocouple
$x$ = distance between thermocouples

$$\therefore T_a-2T_b+T_c+\frac{1}{2m}(T_c-T_a)=\frac{1}{S}(T_{b'}-T_b)$$

$$\therefore T_{b'}-T_b=S(T_a-2T_b+T_c)+\frac{S}{2m}(T_c-T_a)$$

$$\therefore T_{b'}=T_b(1-2S)+S(T_a+T_c)+\frac{S}{2m}(T_c-T_a)$$

$$T_{b'}=T_b(1-2S)+S\left[T_a+T_c+\frac{1}{2m}(T_c-T_a)\right]$$

$$T_{b'}=T_b(1-2S)+S\left[T_a\left(1-\frac{1}{2m}\right)+T_c\left(1+\frac{1}{2m}\right)\right]$$

## References


Ashworth, E. and Ashworth, T. (1980) A simple apparatus for thermal conductivity measurements on rocks under applied stress. *Proceedings of the 20th U.S. Symposium on Rock Mechanics*, Austin, Texas, pp. 27–33.

McPherson, M.J. (1986) The analysis of and simulation of heat flow into underground roadways. *International Journal of Mining and Geological Engineering*, **4**, pp. 000–000.

McPherson, M.J. and Mousset-Jones, P.F. (1984) Background theory to the heat balance at a rock surface, *Proceedings, Second Annual Workshop, Generic Mineral Technology Center Mine Systems Design and Ground Control*, Reno, Nevada, pp. 133–142.

Mousset-Jones, P.F. and McPherson, M.J. (1983) Determination of design parameters for the improved planning of airflow and climate underground, *Proceedings, Annual Workshop, Generic Mineral Technology Center, Mine System Design and Ground Control*, Virginia Polytechnic Institute and State University, pp. 113–142.

Mousset-Jones, P.F. and McPherson, M.J. (1984) Measurement of *in situ* thermal conductivity in an underground mine, *Proceedings, Second Annual Workshop, Generic Mineral Technology Center Mine Systems Design and Ground Control*, Reno, Nevada, pp. 113–131.

Starfield, A.M. *et al.* (1964) The use of computers in heat-flow problems in underground workings. *Colorado School of Mines Quarterly*, **59**, 941–968.

Vost, K.R. (1976) *In situ* measurements of the thermal diffusivity of rock around underground airways. *Transactions of Institution of Mining and Metallurgy*, **85**, A57–A62.